SPATIALLY-LIMITED SAMPLING OF BAND-LIMITED SIGNALS ON THE SPHERE

Wajeeha Nafees[†] *, Zubair Khalid*[†] *, Member, IEEE, and Rodney A. Kennedy*[⋆]*, Fellow, IEEE*

[†] School of Science and Engineering, Lahore University of Management Sciences, Lahore, Pakistan
[⋆] Research School of Engineering, The Australian National University, Canberra, ACT 2601, Australia
Email: 14060020@lums.edu.pk, zubair.khalid@lums.edu.pk, rodney.kennedy@anu.edu.au

ABSTRACT

To support the applications where the measurements can only be taken over spatially limited region on the sphere due to practical limitations, we design a spatially-limited sampling scheme on the sphere for the computation of spherical harmonic transform (SHT) of band-limited signals. By enclosing the inaccessible region with the (anisotropic) ellipsoidal region followed by the rotation of the region to the pole or the equator, we propose an iso-latitude sampling scheme on the sphere. We also present a method to place the samples over the spatially-limited region such that the SHT can be computed accurately. Moreover, we formulate the SHT associated with the proposed sampling scheme and analyse its accuracy through numerical experiments. We also provide an illustration where we reconstruct the head-related transfer function (HRTF) from spatially-limited measurements and demonstrate that the proposed sampling design enables more accurate computation than the existing sampling schemes.

Index Terms— sampling; spherical harmonic transform (SHT); unit sphere; band-limited signals; acoustics

1. INTRODUCTION

Signal analysis on the unit sphere, denoted by $\mathbb{S}^2$, has widespread applications in several fields of science and technology, namely cosmology, geodesy, geomagnetics, acoustics, planetary sciences, etc [1–5]. Signal analysis and processing in these applications is carried out in either spatial (spherical) domain or harmonic (Fourier or spectral) domain that is enabled by the spherical harmonic transform (SHT) which transforms the signal from spatial domain to harmonic domain.

Many sampling schemes and pixelizations on the sphere have been devised in the literature for sampling band-limited signals which result in theoretically exact or accurate computation of the SHT(e.g., see [6–11] and the references therein). All of these sampling schemes require the samples to be taken over the whole sphere. However there are applications where the measurements and samples are available over the spatially-limited region due to practical limitations. For example satellites collecting Earth's data follow an inclined orbit, meaning they cannot take samples near the North and South Pole. This is known as the problem of "polar gap" [12]. In problems related to the measurement of the Earth's gravitational field, we see an unsampled area of about 10° co-latitudinal radius [13]. In an effort to fill in the missing measurements, scientists have recently developed methods for collecting the gravity data over the poles using specially equipped aircrafts [14]. However, the polar gap problem remains largely unsolved in other fields of science. For instance, studies related to geomagnetism indicate that it is better to exclude the data sampled closer than 30° to either pole because they tend to exhibit higher noise contamination as compared to the data sampled near the equator [15]. In cosmology, the sky is considered an analog to the sphere where observations are made from inside out. Hence, we can see only a limited region of the sky from a particular location on Earth [16]. In addition, large portions of the sky remain unobservable owing to the position of the Sun in the Milky Way galaxy and the surrounding stars, gas and dust [17]. Furthermore, the measurements of the head-related transfer function (HRTF) in acoustics in the South polar region (i.e., closer than 36° to the pole) are not considered reliable due to the ground reflections [4, 18].

There exist methods in the literature for the computation of the SHT when the measurements are unavailable or unreliable over the single or double polar cap region. The spherical harmonic basis functions are orthogonal over the sphere. When spatially-limited samples are used for the computation or estimation of the SHT, errors are introduced since the spherical harmonic basis functions no longer remain orthogonal. In other words, the spherical harmonic spectrum suffers from leakage due to the polar gap [19]. In [15], Slepian functions have been used as basis functions for the representation of functions exploiting the orthogonality of Slepian functions over the spatially-limited region. For the accurate computation of the SHT of the HRTF, a novel sampling scheme is proposed in [18] that does not require unreliable measurements samples in the South polar cap for sufficiently accurate computation of the SHT over the band-limits of interest in acoustics.

In this work, we devise a sampling scheme for the computation of the SHT when an arbitrary region on the sphere is inaccessible. Since the ellipsoidal region is anisotropic (directional) in nature, we use it to enclose any arbitrary region on the sphere and develop a sampling scheme for the inaccessible ellipsoidal region on the sphere. We propose iso-latitude sampling where we place rings of samples along co-latitude. Based on the parameters of the ellipsoidal region, we rotate the ellipsoidal region to either polar region or equatorial belt region to maximize the surface area available for the placement of iso-latitude rings of samples. We develop the formulation of the SHT for the proposed sampling scheme and present a method for the placement of iso-latitude rings in such a way that ensures accurate computation of the SHT. We also carry out the accuracy analysis of the SHT associated with the proposed sampling scheme and provide an illustration to demonstrate that the proposed scheme enables more accurate computation of the HRTF than the existing schemes.

The remainder of the paper is compiled as follows. We review the mathematical background and present the problem statement in Section 2. The proposed sampling scheme for spatially-limited sampling of band-limited signals when some region is inaccessible is

Wajeeha Nafees is supported by HEC NRPU Project no. 5925. Zubair Khalid and Rodney A. Kennedy are supported by the Australian Research Council's Discovery Projects funding scheme (Project no. DP170101897).

presented in Section 3, where we also carry out accuracy analysis and provide an illustration. The concluding remarks are then made in Section 4.

2. MATHEMATICAL PRELIMINARIES AND PROBLEM FORMULATION

2.1. Unit Sphere and Regions on the Sphere

A unit-sphere or 2-sphere, denoted by $\mathbb{S}^2$, is defined as $\mathbb{S}^2 \triangleq \left\{\widehat{\boldsymbol{u}} \in \mathbb{R}^3 : \|\widehat{\boldsymbol{u}}\| = 1\right\}$ where $\widehat{\boldsymbol{u}}$ denotes a vector in 3D Euclidean domain and $\|\cdot\|$ is the Euclidean norm. In terms of spherical coordinates, a point on the sphere is parameterized by $\widehat{\boldsymbol{u}} \equiv \widehat{\boldsymbol{u}}(\theta, \phi) \triangleq (\sin\theta\cos\phi, \sin\theta\sin\phi, \cos\theta) \in \mathbb{S}^2$, where $\theta \in [0, \pi]$ denotes the co-latitude and $\phi \in [0, 2\pi)$ denotes the longitude. We also define different types of regions on the sphere which will be used in the subsequent sections. The (South) *polar cap* region, parameterized by co-latitudinal radius θ_p and denoted by $R_p(\theta_p)$, is defined as

$$R_p(\theta_p) \triangleq \{\widehat{\boldsymbol{u}}(\theta, \phi) \in \mathbb{S}^2 | \theta_p \leq \theta \leq \pi, 0 \leq \phi < 2\pi\}, \quad (1)$$

with surface area $|R_p(\theta_p)| = \int_{R_p(\theta_p)} ds(\widehat{\boldsymbol{u}}) = 2\pi(1 - \cos\theta_p)$, where $ds(\widehat{\boldsymbol{u}}) = \sin\theta d\theta d\phi$ represents the differential surface element on $\mathbb{S}^2$.

We also define the *equatorial belt* region of co-latitudinal width $2\theta_e$ as

$$R_e(\theta_e) \triangleq \{(\theta, \phi) | \frac{\pi}{2} - \theta_e \leq \theta \leq \frac{\pi}{2} + \theta_e, 0 \leq \phi < 2\pi\}, \quad (2)$$

and note that $|R_e(\theta_e)| = 4\pi \sin\theta_e$. Lastly, we define an *ellipsoidal* region $R_{\mathcal{E}}(\theta_c, a)$ on the sphere, centered at the North pole, given as

$$R_{\mathcal{E}}(\theta_c, a) \triangleq \left\{\widehat{\boldsymbol{u}}(\theta, \phi) \in \mathbb{S}^2 \,|\, \Delta\left(\widehat{\boldsymbol{u}}, \widehat{\boldsymbol{v}}_1\right) + \Delta\left(\widehat{\boldsymbol{u}}, \widehat{\boldsymbol{v}}_2\right) \leq 2a\right\}, \quad (3)$$

where $\widehat{\boldsymbol{v}}_1 \equiv v_1(\theta_c, 0)$ and $\widehat{\boldsymbol{v}}_2 \equiv v_2(\theta_c, \pi)$ represent the two foci, $\Delta(\widehat{\boldsymbol{u}}, \widehat{\boldsymbol{v}})$ measures the angular distance between two points $\widehat{\boldsymbol{u}}, \widehat{\boldsymbol{v}} \in \mathbb{S}^2$ [20] and a is the length of the semi-major axis aligned with the x-axis. The semi-minor axis of $R_{\mathcal{E}}(\theta_c, a)$ having length b, such that $\Delta\left(\widehat{\boldsymbol{w}}, \widehat{\boldsymbol{v}}_1\right) + \Delta\left(\widehat{\boldsymbol{w}}, \widehat{\boldsymbol{v}}_2\right) = 2a$, is aligned with the y-axis and $\widehat{\boldsymbol{w}} \equiv w(b, \pi/2)$.

2.2. Signals on the Sphere

We consider complex-valued, square integrable functions $h(\widehat{\boldsymbol{u}}) \equiv h(\theta, \phi)$ on $\mathbb{S}^2$, which form a complete Hilbert space $L^2(\mathbb{S}^2)$ equipped with the inner product

$$\langle h_1, h_2 \rangle \triangleq \int_{\mathbb{S}^2} h_1(\theta, \phi)\overline{h_2(\theta, \phi)} \sin\theta \, d\theta \, d\phi, \quad (4)$$

for any two functions $h_1,\ h_2$ defined on $\mathbb{S}^2$, $\overline{(\cdot)}$ denotes the complex conjugate operation and $\int_{\mathbb{S}^2} = \int_{\theta=0}^{\pi}\int_{\phi=0}^{2\pi}$. The inner product in (4) induces a norm $\|h\| \triangleq \langle h, h\rangle^{1/2}$. Functions with finite energy (or induced norm) are referred to as "signals on the sphere".

2.3. Spherical Harmonic Transform

For the Hilbert space $L^2(\mathbb{S}^2)$, the spherical harmonic functions, denoted by $Y_\ell^m(\theta, \phi)$ for degree $\ell \geq 0$ and order $-\ell \leq m \leq \ell$, form a set of complete, orthonormal basis functions and therefore, any function $h \in L^2(\mathbb{S}^2)$ can be expanded as

$$h(\theta, \phi) = \sum_{\ell=0}^{\infty}\sum_{m=-\ell}^{\ell} (h)_\ell^m Y_\ell^m(\theta, \phi), \quad (5)$$

where

$$(h)_\ell^m \triangleq \langle h, Y_\ell^m\rangle = \int_{\mathbb{S}^2} h(\theta, \phi)\overline{Y_\ell^m(\theta, \phi)} \sin\theta \, d\theta \, d\phi, \quad (6)$$

is the spherical harmonic coefficient of degree ℓ and order m. The spherical harmonic coefficients form the harmonic (spectral) domain representation of the signal h. Equations (6) is referred to as the spherical harmonic transform (SHT) and (5) is the inverse SHT. For a signal $h \in L^2(\mathbb{S}^2)$ band-limited at L such that $(h)_\ell^m = 0\ \forall \ell \geq L$, the summation in (5) over ℓ is truncated at $L-1$. These band-limited signals form a subspace, denoted by $\mathcal{H}_L$, of dimensionality L^2.

2.4. Rotation on the Sphere

We define the rotation operator $\mathcal{D}(\alpha, \beta, \gamma)$ that rotates a function on the sphere, following the 'zyz' Euler convention, in the sequence of $\gamma \in [0, 2\pi)$ rotation around z-axis, $\beta \in [0, \pi]$ rotation around y-axis and $\alpha \in [0, 2\pi)$ rotation around z-axis. The effect of the rotation operator on the signal $h \in L^2(\mathbb{S}^2)$ can be realized as the inverse rotation of the coordinates, that is,

$$\big(\mathcal{D}(\alpha, \beta, \gamma)h\big)(\widehat{\boldsymbol{u}}) = h(\boldsymbol{R}^{-1}\widehat{\boldsymbol{u}}) \quad (7)$$

where $\boldsymbol{R}$ is the rotation matrix associated with the rotation operator $\mathcal{D}(\alpha, \beta, \gamma)$ [20] and therefore depends on the rotation parameters α, β, γ. We also note that the spherical harmonic coefficients of the original signal h and the rotated signal $\mathcal{D}(\alpha, \beta, \gamma)h$ are related by

$$(\mathcal{D}(\alpha, \beta, \gamma)h)_\ell^m = \sum_{m'=-\ell}^{\ell} D_{m,m'}^\ell(\alpha, \beta, \gamma)(h)_\ell^{m'}, \quad (8)$$

where $D_{m,m'}^\ell(\alpha, \beta, \gamma)$ denotes the Wigner-D function [20].

2.5. Problem Under Consideration

Spherical signal processing techniques analyse signals in both the spatial and spectral domains. To extract spectral information of a signal, the spherical harmonic transform (SHT) given in (6) computes the spherical harmonic coefficients using samples of the signal in spatial domain. Sampling schemes have been proposed which lead to either theoretically exact or accurate computation of the SHT. All of these schemes assume that samples are available on the entire sphere. However, there are applications where samples cannot be taken over some region, for instance, the polar gap problem in geodesy [15], south polar cap region in HRTF measurements [4] and SDSS DR7 quasar binary mask in cosmology [21]. In this paper, we consider a problem to compute the SHT when some region on the sphere is inaccessible. By enclosing the inaccessible region within an ellipsoidal region, followed by the rotation of the ellipsoidal region either to a polar cap region or the equatorial belt region, we propose spatially-limited iso-latitude sampling on the sphere for the computation of the SHT.

3. SPATIALLY-LIMITED SAMPLING ON THE SPHERE

3.1. Sampling Design - Inaccessible Ellipsoidal Region

We first devise a sampling scheme on the sphere when the ellipsoidal region $R_{\mathcal{E}}^{'}(\theta_c, a)$ is inaccessible. We later take into account the arbitrary shaped region by enclosing it with the ellipsoidal region. We propose to take iso-latitude rings of samples of the band-limited signal $h \in \mathcal{H}_L$ on the sphere over the accessible region. For the inaccessible ellipsoidal region $R_{\mathcal{E}}^{'}(\theta_c, a)$, the iso-latitude rings of samples of the signal h can be taken on $\mathbb{S}^2 \backslash R_p(a)$ and therefore the surface area available for sampling is $4\pi - |R_p(a)| = 2\pi(1 + \cos a)$.

If we rotate the signal and inaccessible ellipsoidal region by $\pi/2$ along z-axis and then by $\pi/2$ along y-axis, its semi-major and minor axes get aligned with the y-axis and z-axis respectively and the iso-latitude rings of samples of the *rotated* signal $\mathcal{D}(0, \pi/2, \pi/2)h$ can now be taken on $\mathbb{S}^2 \backslash R_e(b)$ of surface area $4\pi(1 - \sin b)$. If $(1+\cos a) > 2(1-\sin b)$ for a given inaccessible ellipsoidal region $R_{\mathcal{E}}^{'}(\theta_c, a)$, we rotate the signal prior to sampling such that the major axis of the inaccessible ellipsoidal region is aligned with the y-axis as such judicious choice ensures the availability of larger area for the sampling of the signal. With this consideration, we propose to take L iso-latitude rings of samples at locations such that $\theta_k \in \Theta$ where

$$\Theta = \begin{cases} \theta \in [0, \pi - a] & (1 + \cos a) < 2(1 - \sin b) \\ \theta \in [0, \frac{\pi}{2} - b] \cup [\frac{\pi}{2} + b, \pi] & \text{otherwise.} \end{cases} \tag{9}$$

For a ring placed at θ_k, we take $2k+1$ equally spaced points along ϕ. Before we present a method to determine the ring locations θ_k, $k = 0, 1, \ldots, L-1$ such that the SHT of the band-limited signal can be computed accurately, we first review the formulation of the spherical harmonic transform [11].

3.2. SHT Formulation

Define a vector $\boldsymbol{h}_m$ of spherical harmonic coefficients of angular order $|m| < L$, such that

$$\boldsymbol{h}_m = \left[(h)^m_{|m|}, (h)^m_{|m|+1}, \ldots, (h)^m_{L-1}\right]^T, \tag{10}$$

and a matrix $\boldsymbol{P}_m$ of dimension $(L-|m|) \times (L-|m|)$ with elements given by

$$\boldsymbol{P}_m(k, j) = Y^m_{|m|+j-1}(\theta_{|m|+k-1}, 0), \quad k, j = 1, 2, \ldots, L - |m|. \tag{11}$$

Also define a vector $\boldsymbol{f}_m$ for each order $|m| < L$ as

$$\boldsymbol{f}_m \triangleq \left[F_m(\theta_{|m|}), F_m(\theta_{|m|+1}), \ldots, F_m(\theta_{L-1})\right]^T, \tag{12}$$

such that

$$F_m(\theta_k) \triangleq \int_0^{2\pi} h(\theta_k, \phi) e^{-im\phi} d\phi = 2\pi \sum_{\ell=|m|}^{L-1} (h)^m_\ell Y^m_\ell(\theta_k, 0), \tag{13}$$

where the second equality follows from (5) and the orthogonality of the complex exponentials.

Noting the structure of $F_m(\theta_k)$ in (13), we can write

$$F_m(\theta_k) = \boldsymbol{P}_m(k, :)\, \boldsymbol{h}_m, \tag{14}$$

which implies that

$$\boldsymbol{f}_m = \boldsymbol{P}_m \boldsymbol{h}_m. \tag{15}$$

3.3. Placement of Iso-latitude Rings

The vector $\boldsymbol{h}_m$ containing the SHT coefficients of order m can be recovered by solving a system of linear equations provided $\boldsymbol{P}_m$ is well-conditioned and $\boldsymbol{f}_m$ can be computed correctly. For the proposed sampling scheme, $F_m(\theta_k)$ for $k = |m|, |m+1|, \ldots, L-1$ can be computed correctly by employing FFT as we have taken $2k+1$ samples along ϕ on a ring placed at θ_k [11]. We use the following method to determine the optimal location of L iso-latitude rings, that is $\theta_k, k = 0, 1, \ldots, L-1$, in a spatially limited region ($\theta_k \in \Theta$) such that the matrix $\boldsymbol{P}_m$ given in (11) is well-conditioned for each m.

- Consider a set of $N \gg L$ equiangular points taken over Θ.
- Choose the θ_{L-1} from Θ as the point farthest away from the poles ($\theta = 0$ or $\theta = \pi$).
- For $k = L-2, L-3 ..., 1, 0$, choose θ_k from the remaining elements of Θ for which the condition number of the matrix $\boldsymbol{P}_m$ defined in (11) is minimum.

Determining the location of the rings by using the method described above ensures well-conditioning of $\boldsymbol{P}_m$ matrix for every m. Consequently, the spherical harmonic transform can be accurately computed by solving the system given in $\boldsymbol{f}_m = \boldsymbol{P}_m \boldsymbol{h}_m$ for each $|m| = 0, 1 \ldots, L-1$. For the case when the ellipsoidal region and the signal are rotated to align the inaccessible region along equatorial belt region, we recover, through SHT, the coefficients of the rotated signal $\mathcal{D}(0, \pi/2, \pi/2)h$ which we can use in (8) to obtain the SHT of the signal h.

3.4. Multi-pass SHT

To further improve the accuracy of the computation of the SHT from the samples over the spatially limited region, we use a multi-pass algorithm [22]. For a signal $h(\theta, \phi)$ in the spatial domain, we obtain the spherical harmonic coefficients $(h_k)^m_\ell$ and re-synthesize the signal as $\tilde{h}_k(\theta, \phi) = \sum_{\ell=0}^{L-1} \sum_{m=-\ell}^{\ell} (h_k)^m_\ell Y^m_\ell(\theta, \phi)$, where k indicates the iteration number. The residual between $h(\theta, \phi)$ and $\tilde{h}_k(\theta, \phi)$ is calculated as

$$r_k(\theta, \phi) = h(\theta, \phi) - \tilde{h}_k(\theta, \phi). \tag{16}$$

The spherical harmonic coefficients of the residual, denoted by $(r_k)^m_\ell$, are then computed and used to update the spherical harmonic coefficients of the signal as

$$(h_{k+1})^m_\ell = (h_k)^m_\ell + (r_k)^m_\ell. \tag{17}$$

We repeat this process until the stopping criterion: $r_k(\theta, \phi) > r_{k-1}(\theta, \phi)$.

3.5. Inaccessible Arbitrary Region

We have devised the sampling scheme when ellipsoidal region is inaccessible on the sphere. For the case when an arbitrary shaped region $R \subset \mathbb{S}^2$ is inaccessible, we propose to rotate the signal and the region R such that the region R is enclosed by the ellipsoidal region $R_{\mathcal{E}}(\theta_c, a)$, where we choose rotation parameters and ellipsoidal region parameters which ensure that $R_{\mathcal{E}} \cap R = R$ and $|R_{\mathcal{E}} - R|$ is minimized.

3.6. Accuracy Analysis

We here analyse the numerical accuracy of the proposed spatially-limited sampling scheme on the sphere and the associated multi-pass SHT. In order to analyse the accuracy, we carry out numerical experiments where we obtain a band-limited test signal $h_t \in \mathcal{H}_L$ by randomly generating its spherical harmonic coefficients $(h_t)^m_\ell$ with uniform distribution in the interval $[-1, 1]$ for both the real and imaginary parts and then synthesizing a signal h_t over the proposed sampling scheme when the ellipsoidal region $R_{\mathcal{E}}(\theta_c, a)$ is inaccessible. We use multi-pass SHT to recover the spherical harmonic coefficients denoted by $(h_r)^m_\ell$ and compute the mean error given by

$$E_{\text{mean}} \triangleq \frac{1}{L^2} \sum_{\ell=0}^{L-1} \left| (h_t)^m_\ell - (h_r)^m_\ell \right|, \tag{18}$$

which is averaged over 10 realizations of the experiment and plotted for the band-limit $L = 32$, semi-major axis length $a = 2\pi/10$, $3\pi/20$ and $\pi/10$ and different values of the flattening $0 \leq f \triangleq \frac{a-b}{a} \leq 1$ of the ellipsoidal region in Fig. 1, where it can observed

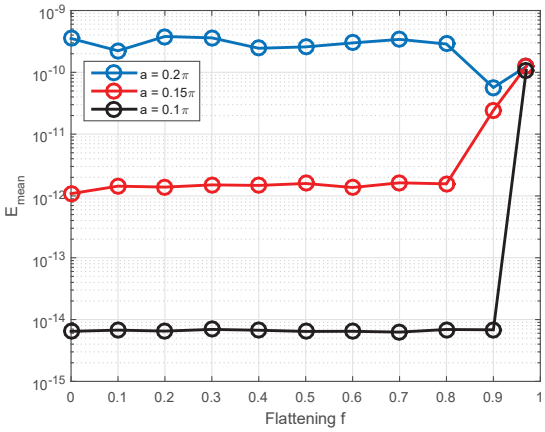

Fig. 1: Mean error observed when flattening varies in the range $0 \leq f < 1$ for a constant band-limit $L = 32$ and semi-major axis $a = 0.2\pi, 0.15\pi$ and 0.1π.

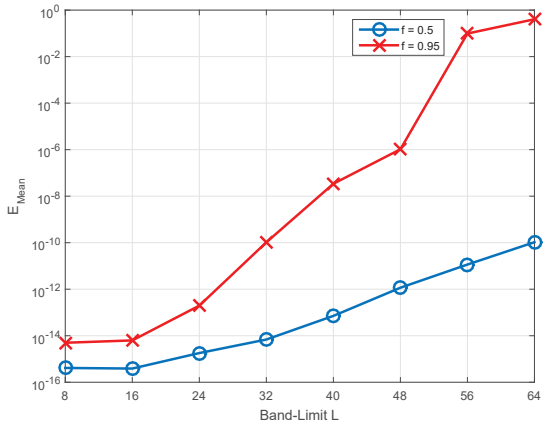

Fig. 2: Mean error observed when ellipse remains at the North pole ($f = 0.5$) and when it is rotated to the equatorial belt ($f = 0.95$) as band-limit varies in the range $8 \leq L \leq 64$. Here $a = 0.1\pi$

that the rotation of the ellipsoidal region to the equatorial belt region enables accurate reconstruction for the larger values of f (directional ellipsoidal region). For the smaller values of f, the reconstruction error is smaller if the ellipsoidal region is not rotated which is due to the fact that the surface area for sampling is larger when the ellipsoidal region of smaller f is enclosed by the polar cap region than the equatorial belt region. We also extend our analysis and plot the mean error E_{mean} in Fig. 2 for different band-limits $8 \leq L \leq 64$, semi-major axis length $a = \pi/10$ and two values of flattening $f = 0.5$ (when the ellipsoidal region remains at the North pole) and $f = 0.95$ (when the ellipsoidal region is rotated to the equatorial belt). Accuracy analysis reveals that the proposed sampling design on the sphere enables accurate computation of the SHT when the samples of the band-limited signal are inaccessible over some region on the sphere. For a given inaccessible region $R \subset \mathbb{S}^2$, we note that the bounds on the reconstruction error can be obtained by taking into account the surface area $4\pi - |R|$ available for sampling and the signal band-limit L. However, it is the subject of future work.

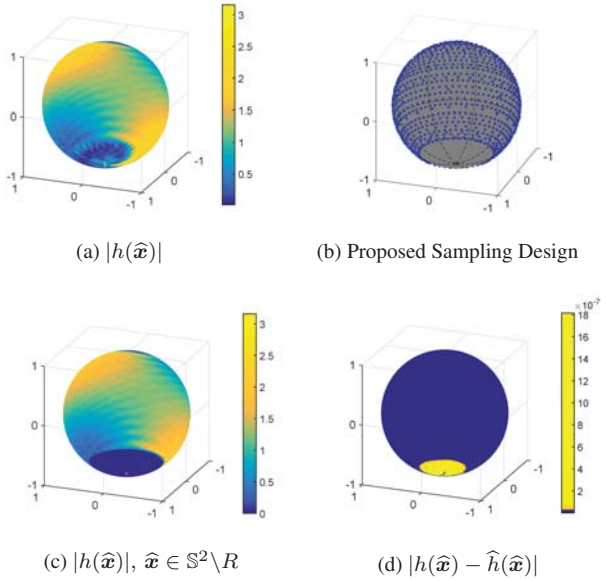

(a) $|h(\widehat{\boldsymbol{x}})|$ (b) Proposed Sampling Design

(c) $|h(\widehat{\boldsymbol{x}})|$, $\widehat{\boldsymbol{x}} \in \mathbb{S}^2 \backslash R$ (d) $|h(\widehat{\boldsymbol{x}}) - \widehat{h}(\widehat{\boldsymbol{x}})|$

Fig. 3: HRTF signal (a) $|h|$, (b) the proposed sampling points for $L = 32$, (c) the known signal $|h|$ and (d) the reconstruction error $|h - \widehat{h}|$.

3.7. Illustration

Here we use the proposed sampling scheme and the associated multi-pass SHT algorithm for the computation of the SHT of the signal obtained from the analytical HRTF model [23]. The following parameters are used in the model to obtain the HRTF signal h: head radius $a = 0.09$ m, distance from the center of the sphere to the source $r = 1$ m, sound frequency $f_s = 15$ kHz and speed of sound $c = 340$ m/s. Since the HRTF measurements are unreliable at the South polar region, we design the sampling scheme for the region $R = \{(\theta, \phi) | 0 \leq \theta \leq 8\pi/10, 0 \leq \phi < 2\pi\}$ for band-limit $L = 38$. We then use multi-pass SHT algorithm to obtain the reconstructed signal $\widehat{h}$. We plot the absolute value of the signal $|h|$, sampling points of the proposed scheme over the accessible region, samples of the signal $|h|$ and the error $|h - \widehat{h}|$ in Fig. 3, where it can be observed that the proposed sampling scheme enables the accurate reconstruction, with error on the order of 10^{-7}, over the inaccessible region.

4. CONCLUSIONS

In this work, we propose a spatially-limited sampling scheme for the computation of spherical harmonic coefficients (using a multi-pass SHT algorithm) of a band-limited signal when an arbitrary region on the sphere is inaccessible for taking signal measurements or samples. We propose to place iso-latitude rings of samples on the sphere after the exclusion of the minimum area ellipsoidal region enclosing the inaccessible region. Prior to sampling, the ellipsoidal region may be rotated to the polar cap or the equatorial belt depending upon the surface area available for placement of samples in each case. Placement of the rings according to the proposed method results in accurate computation of the SHT. The numerical accuracy of the proposed sampling scheme was analysed and gives promising results. As an illustration we compute the SHT of the HRTF signal using the proposed spatially-limited sampling method and note that its accuracy has improved as compared to the existing schemes.

5. REFERENCES

[1] M. Tegmark, M. A. Strauss, M. R. Blanton, K. Abazajian, S. Dodelson, H. Sandvik, X. Wang, D. H. Weinberg, I. Zehavi, N. A. Bahcall *et al.*, "Cosmological parameters from sdss and wmap," *Physical Review D*, vol. 69, no. 10, p. 103501, 2004.

[2] M. A. Wieczorek and F. J. Simons, "Minimum variance multitaper spectral estimation on the sphere," *J. Fourier Anal. Appl.*, vol. 13, no. 6, pp. 665–692, 2007.

[3] F. Lowes, "Spatial power spectrum of the main geomagnetic field, and extrapolation to the core," *Geophysical Journal International*, vol. 36, no. 3, pp. 717–730, 1974.

[4] W. Zhang, M. Zhang, R. A. Kennedy, and T. D. Abhayapala, "On high-resolution head-related transfer function measurements: An efficient sampling scheme," *IEEE Trans. Acoust., Speech, Signal Process.*, vol. 20, no. 2, pp. 575–584, 2012.

[5] M. A. Wieczorek, "Gravity and topography of the terrestrial planets," *Treatise on geophysics*, vol. 10, no. 206, pp. 165–989, 2007.

[6] J. R. Driscoll and D. M. Healy, Jr., "Computing Fourier transforms and convolutions on the 2-sphere," *Adv. Appl. Math.*, vol. 15, no. 2, pp. 202–250, Jun. 1994.

[7] A. G. Doroshkevich, P. D. Naselsky, O. V. Verkhodanov, D. I. Novikov, V. I. Turchaninov, I. D. Novikov, P. R. Christensen, and Chiang, "Gauss Legendre Sky Pixelization (GLESP) for CMB maps," *Int. J. Mod. Phys. D.*, vol. 14, no. 02, pp. 275–290, Feb. 2005.

[8] J. D. McEwen and Y. Wiaux, "A novel sampling theorem on the sphere," *IEEE Trans. Signal Process.*, vol. 59, no. 12, pp. 5876–5887, Dec. 2011.

[9] K. M. Górski, E. Hivon, A. J. Banday, B. D. Wandelt, F. K. Hansen, M. Reinecke, and M. Bartelmann, "HEALPix: A Framework for High-Resolution Discretization and Fast Analysis of Data Distributed on the Sphere," *Astrophys. J.*, vol. 622, pp. 759–771, Apr. 2005.

[10] J. Blais and M. Soofi, "Spherical harmonic transforms using quadratures and least squares," in *Computational Science ICCS 2006*, ser. Lecture Notes in Computer Science. Springer Berlin Heidelberg, 2006, vol. 3993, pp. 48–55.

[11] Z. Khalid, R. A. Kennedy, and J. D. McEwen, "An optimal-dimensionality sampling scheme on the sphere with fast spherical harmonic transforms," *IEEE Transactions on Signal Processing*, vol. 62, no. 17, pp. 4597–4610, 2014.

[12] C. Tscherning, R. Forsberg, A. Albertella, F. Migliaccio, and F. Sanso, "The polar gap problem," *Space-wise approaches to gravity field determination in Polar areas, Eotvos to mGal, Finsal report*, vol. 10, pp. 331–336, 2000.

[13] F. G. Lemoine, N. K. Pavlis, S. C. Kenyon, R. H. Rapp, E. Pavlis, and B. Chao, "New high-resolution model developed for earth's gravitational field," *Eos, Transactions American Geophysical Union*, vol. 79, no. 9, pp. 113–118, 1998.

[14] R. Forsberg, A. Olesen, F. Ferraccioli, T. Jordan, and K. Matsuoka, "Airborne geophysical surveys of unexplored regions of antarctica-results of the esa polargap campaign," in *AGU Fall Meeting Abstracts*, 2016.

[15] F. J. Simons and F. Dahlen, "Spherical slepian functions and the polar gap in geodesy," *Geophysical Journal International*, vol. 166, no. 3, pp. 1039–1061, 2006.

[16] M. Tegmark, "A method for extracting maximum resolution power spectra from microwave sky maps," *Monthly Notices of the Royal Astronomical Society*, vol. 280, no. 1, pp. 299–308, 1996.

[17] G. Lewsi. (2014, Aug.) Cosmic radiation: the dawn of new physics or statistical slip-up? [Online]. Available: https://phys.org/news/2014-08-cosmic-dawn-physics-statistical-slip-up.html

[18] A. P. Bates, Z. Khalid, and R. A. Kennedy, "Novel sampling scheme on the sphere for head-related transfer function measurements," *IEEE/ACM Transactions on Audio, Speech and Language Processing (TASLP)*, vol. 23, no. 6, pp. 1068–1081, 2015.

[19] N. Sneeuw and M. Van Gelderen, "The polar gap," in *Geodetic boundary value problems in view of the one centimeter geoid*. Springer, 1997, pp. 559–568.

[20] R. A. Kennedy and P. Sadeghi, *Hilbert Space Methods in Signal Processing*. Cambridge, UK: Cambridge University Press, Mar. 2013.

[21] Z. Khalid, R. A. Kennedy, and J. D. McEwen, "Slepian spatial-spectral concentration on the ball," *arXiv preprint arXiv:1403.5553*, 2014.

[22] W. Nafees, Z. Khalid, R. A. Kennedy, and J. D. McEwen, "Optimal-dimensionality sampling on the sphere: Improvements and variations," in *Sampling Theory and Applications (SampTA), 2017 International Conference on*. IEEE, 2017, pp. 87–91.

[23] R. O. Duda and W. L. Martens, "Range-dependence of the hrtf for a spherical head," in *Proceedings of 1997 Workshop on Applications of Signal Processing to Audio and Acoustics*, Oct 1997, pp. 5 pp.–.